chemistry proceedings

MDPI

Proceeding Paper

Synthesis of Peptide-NSAID Hybrid Compounds and Their Selectivity in Inhibiting the Dual COX-LOX System Described Through Docking and Molecular Dynamics †

Juan C. Jiménez-Cruz [1], Ramón Guzmán-Mejía [2], Pedro Navarro-Santos [1,*], Hugo A. García Gutiérrez [2], Julio Cesar Ontiveros-Rodriguez [2], Rafael Herrera-Bucio [2] and Judit A. Aviña-Verduzco [2,*]

[1] CONAHCyT-Universidad Michoacana de San Nicolás de Hidalgo, Edificio B-1, Ciudad Universitaria, Morelia 58030, Michoacán, Mexico; 0451324h@umich.mx (J.C.J.-C.)
[2] Francisco J. Múgica, Instituto de Investigaciones Químico Biologicas, Universidad Michoacana de San Nicolás de Hidalgo, Morelia 58030, Michoacán, Mexico; ramon.guzman@umich.mx (R.G.-M.); hgarcia@umich.mx (H.A.G.G.); julio.ontiveros@umich.mx (J.C.O.-R.); rafael.herrera.bucio@umich.mx (R.H.-B.)
* Correspondence: pedro.navaro@umich.mx (P.N.-S.); jaavina@umich.mx (J.A.A.-V.), Tel.: +52-(443)-326-5788
† Presented at the 28th International Electronic Conference on Synthetic Organic Chemistry (ECSOC 2024), 15–30 November 2024; Available online: https://sciforum.net/event/ecsoc-28.

Abstract: The synthesis of compounds based on a hybrid structure combining a fenbufen analog (a nonsteroidal anti-infammatory drug, NSAID) with amino acids or peptides is described. Additionally, detailed molecular docking analysis was performed to investigate their drug-receptor interactions with inflammation-related enzymes COX-2 and 5-LOX. The hybrid compound that demonstrated the best interaction was further evaluated through molecular dynamics simulations, and its binding free energy (ΔG) was calculated using the Molecular Mechanics Poisson-Boltzmann Surface Area (MMPBSA) method.

Keywords: NSAID; MMPBSA; PEPTIDES; COX/LOX

Citation: Jiménez-Cruz, J.C.; Guzmán-Mejía, R.; Navarro-Santos, P.; Gutiérrez, H.A.G.; Ontiveros-Rodriguez, J.C.; Herrera-Bucio, R.; Aviña-Verduzco, J.A. Synthesis of Peptide-NSAID Hybrid Compounds and Their Selectivity in Inhibiting the Dual COX-LOX System Described Through Docking and Molecular Dynamics. *Chem. Proc.* **2024**, *6*, x. https://doi.org/10.3390/xxxxx

Academic Editor(s): Name

Published: 15 November 2024

1. Introduction

Inflammation is an immune response to harmful agents, biochemically characterized by the production of pro-inflammatory cytokines such as interleukins (IL) IL-1, IL-2, IL-6, IL-7, and tumor necrosis factor-alpha (TNFα) [1]. These interleukins are also overexpressed in globally relevant infections, such as COVID-19, where enzymes like cyclooxygenase-2 (COX2) [2] y 5-lipoxygenase (5-LOX) [3] are likewise upregulated, contributing to increased severity. Another condition where these enzymes are also overexpressed is rheumatoid arthritis, where the resulting metabolites stimulate the production of pro-inflammatory cytokines such as IL-1, IL-6, and IL-8, among others [4]. Given the global prevalence of rheumatoid arthritis, estimated at 0.46% between 1980 and 2018 [5], recent research has focussed on treating inflammation through the use of selective COX-2/5-LOX inhibitors [6], yielding promising results in diseases like cancer [7]. One approach to achieving dual inhibition systems has been the selection of nonsteroidal anti-inflammatory drugs (NSAIDs) conjugated with amino acids (AAs) or peptides. In this context, small peptides have shown potent inhibitory activity against the COX-2 isoenzyme, particularly tripeptides reported by Rajakrishnan et al., which exhibit inhibition values comparable to celecoxib [8]. Furthermore, peptides isolated from wheat have been shown to have a protective effect reducing intestinal damage and cytokine levels when administered alongside NSAIDs, as described by Yin et al. [9]. Ionic salts of NSAID-AA conjugates [10] have also been explored for their potential to inhibit inflammation and viral replication in virus SARS-CoV-2 [11]. These conjugates have been synthesized either with linkers [12] or

through covalent bonds [13]. Moreira et al. [14] reported a series of naproxen (Npx)-dehydrodipeptide hybrids, where AAs served as central linkers or C-terminal residues, with inhibition values against 5-LOX comparable to naproxen. Among these, the Npx-*L*-Ala-Z-ΔPhe-OH hybrid was identified as a lead compound. Li et al. [15] using naproxen as the base, coupled aromatic *D*-AAs to achieve selectivity ratios of 20:1. Additionally, they conjugated other NSAIDs such as (*R*)-furbiprofen, (*R*,*S*)-furbiprofen, (*R*,*S*)-ibuprofen, forming supramolecular gel aggregates that exhibited strong COX inhibition [16]. Finally, naproxen has been conjugated with other amino acids and their methyl esters, yielding hydrophobic compounds designed to enhance interaction with the enzyme's binding pocket, thereby improving catalytic cavity interactions [17].

2. Results and Discussion

In this study, the synthesis of four novel hybrid NSAID-AA and NSAID-peptide compounds is described, based on the conjugation of the fenbufen analog, 4-(4-methoxyphenyl)-4-oxobutanoic acid, obtained through a Heck cross-coupling reaction between 2,3-DHF and 4-iodoanisole [18]. The synthesis followed is outlined in Scheme 1, starting with the coupling of *L*-phenylalanine (Phe) and *L*-tyrosine (Tyr) esters to the aryl keto-ester fenbufen analog, using isobutyl chloroformate as the coupling agent. This coupling reaction yielded compounds **1** and **2**, subsequently subjected to basic hydrolysis to produce the free acids **3** and **4**. These acids were then coupled with an additional residue of amino esters derived from Phe and Tyr, resulting in the final hybrid NSAID-dipeptide compounds, methyl (4-(4-methoxyphenyl)-4-oxobutanoyl)-*L*-tyrosyl-*L*-tyrosinate (**5**), methyl (4-(4-methoxyphenyl)-4-oxobutanoyl)-*L*-phenylalanyl-*L*-tyrosinate (**6**), methyl (4-(4-methoxyphenyl)-4-oxobutanoyl)-*L*-tyrosyl-*L*-phenylalaninate (**7**) y methyl (4-(4-methoxyphenyl)-4-oxobutanoyl)-*L*-phenylalanyl-*L*-phenylalaninate (**8**). As observed, the peptide fragment in hybrids **5–8** exists in the methyl ester form, aimed at reducing the compounds' polarity and improving their solubility and transdermal absorption. Once the hybrid compounds **3–8** were synthesized and elucidated, molecular docking studies were conducted with the COX-2 (3LN1) y 5-LOX (3O8Y) enzymes. For COX-2, a redocking process was performed to validate the molecular docking method, yielding an RMSD of 0.91 Å for celecoxib (Cel), indicating an accurate method as the obtained pose closely matched the crystal pose. For 5-LOX, since no co-crystallized reference drug was available, it was docked with the selective inhibitor zileuton. The molecular docking binding results for COX-2 and 5-LOX are presented in Tables 1 and 2.

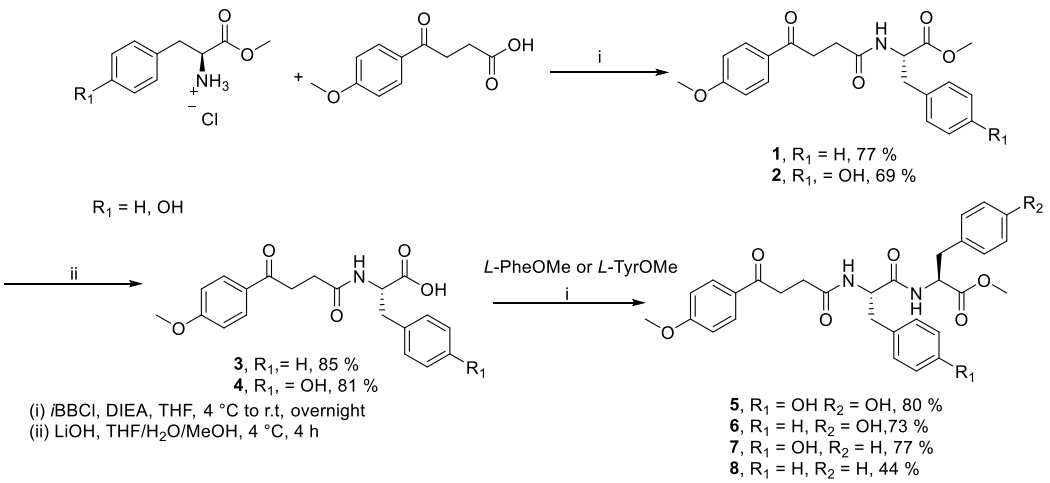

Scheme 1. Synthesis pathway of the hybrid peptide-NSAID compounds **5–8**.

Table 1. The binding energy of compounds **3–8** with COX-2 and 5-LOX.

			Compound					
Entry	**Protein**	**Reference**	**3**	**4**	**5**	**6**	**7**	**8**
1	COX2 (kcal/mol)	−11.01 (celecoxib)	−10.38	−9.49	−10.09	−11.10	−11.01	**−10.57**
2	5LOX (kcal/mol)	−7.83 (zileuton)	−9.06	−9.05	−6.89	−9.2	−7.3	−8.90

Docking analysis with the 3LN1 protein revealed that compounds **3**, **6**, **7**, and **8** showed interaction values similar to the selective COX-2 inhibitor. A noteworthy finding across all assays was the presence of both polar and hydrophobic interactions with the VAL-509 residue, which is considered crucial for the selective inhibition of the COX-2 isoenzyme. A detailed analysis indicated that the best interaction energies were observed with compounds **6** (11.10 kcal/mol) and **7** (11.01 kcal/mol). In both cases, the ligands adopt a folded, helix-like conformation with their aromatic rings exposed to the hydrophobic catalytic cavity. Specifically for compound **7** (TyrPhe residue), the hydroxyl group of the Tyr residue is oriented toward a region containing polar residues; this group participates in three hydrogen bonds with residues GLN-178 (2.29 Å), LEU-338 (3.07 Å) y PHE-504 (2.49 Å), interactions commonly found in COXIB-type NSAIDs (Figure 1a,b). Moreover, a comparative analysis of the docking poses between compound **7** and celecoxib showed a remarkably similar folded conformation, with the Tyr hydroxyl group directed toward the same region as the celecoxib sulfonamide group (Figure 1c).

For 5-LOX, compounds **3** and **4** exhibited affinity values exceeding −9 kcal/mol, higher than zileuton. In the lipoxygenase complexes, compound **3** displayed two notable hydrogen bonds: the first with HIS-367 (2.16 Å), an AA chelated to a Fe^{+2} atom, and the second with ALA-424 (2.58 Å), a hydrogen bond also associated with zileuton interactions. In the case of compound **4**, the ligand is positioned near the Fe atom, approaching it via the hydroxyl group of Tyr, forming a hydrogen bond with the C-terminal carboxylate of ILE-673; which is also coordinated to the catalytic Fe atom through a metal bond. This interaction could potentially disrupt the coordination sphere around the metal, as the COO^- anion is inserted into the helical region, possibly inactivating the protein. In addition, three hydrogen bonds were identified along the ligand groove with residues GLN-363, THR-364, and ALA-424. An unconventional hydrogen bond (2.68 Å) was also observed between the π-cloud of the anisole ring and ASN-425 (Figure 1d,e). In this context, the adopted pose is stabilized by nonpolar alkyl and π-alkyl interactions. In the comparative analysis with zileuton, both compounds display a characteristic U-shaped conformation, where the anisole ring is oriented similarly to the benzothiophene ring, and the amide bond of compound **4** is positioned similarly to the hydroxyl urea group present in the 5-LOX inhibitor (Figure 1f).

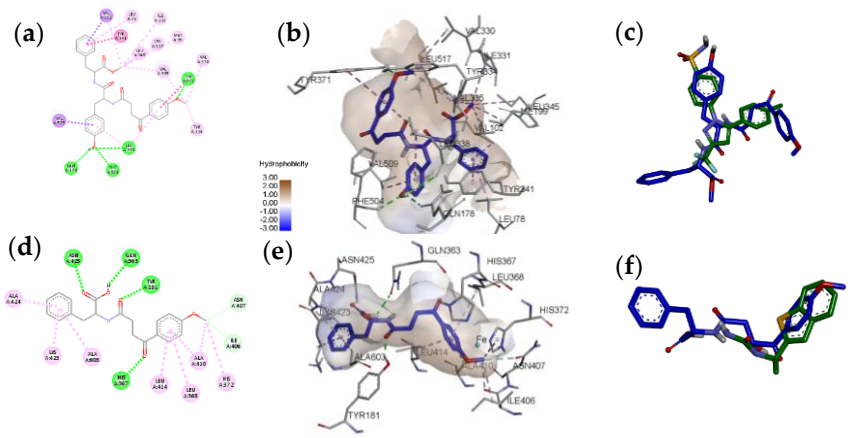

Figure 1. (**Top**) Interactions of COX-2 and compound **7** in (**a**) 2D, (**b**) 3D, and (**c**) comparison of celecoxib and compound **7**. (**Bottom**) Interactions of 5-LOX and compound **4** in (**d**) 2D, (**e**) 3D, and (**f**) comparison of zileuton and compound **4**.

Afterward, the best result from the COX-2 docking study was subjected to a 100 ns molecular dynamics simulation to assess the stability and evolution of the complex over time, calculating the root mean square deviation (RMSD). The average RMSD for the protein backbone was 1.774 Å, with minimum values of 0.699 Å and maximum fluctuations reaching 2.587 Å. For the ligand, the average RMSD was 1.326 Å, with minimum values of 0.460 Å and maximum values of 2.294 Å. This finding is significant, as the observed values indicate a high stability of ligand **7** within the catalytic site, achieved after 20 ns of simulation. Part of this stability can be explained by the hydrogen bonds observed during most of the simulation, with H-bonds formed with SER-516 (occupancy of 52.12% throughout the simulation), as well as TYR-334 (75.88%) and VAL-74 (38.34%). Additional information indicates that the binding free energy (ΔG_{bind}) was determined using the MMPBSA method, where the complex showed an energy of −33.91 kcal/mol. Although this energy is higher than the previously reported value for celecoxib (−47 kcal/mol or −198 kJ/mol) [19], it is still promising, considering is being compared to one of the best COX-2 inhibitors. The wide energetic contributions attributed to Van der Waals (−59.99 kcal/mol) and electrostatic interactions (−34.13 kcal/mol) are both consistent with the largely nonpolar nature of the catalytic site.

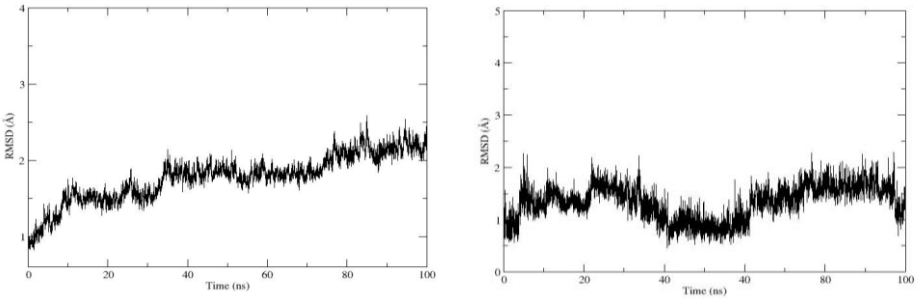

Figure 2. RMSD of (**a**) compound **7** with the backbone of protein α and (**b**) RMSD as a function of the ligand.

3. Experimental Section

3.1. General

Column chromatography was carried out with Merck Silica Gel (70–230 mesh). TLC was performed with Merck 60-F25 plates, and spots were visualized using UV light and iodine vapor. Melting points were measured with a Fischer model 1237 apparatus and are uncorrected. NMR spectra were recorded on a Varian Mercury plus (100 and 400 MHz).

3.2. Computational Details

Molecular docking was conducted with the COX-2 (PDB ID: 3LN1) and 5-LOX stable (PDB ID: 3O8Y) proteins. Water molecules and additional ligands were removed from each protein subunit, and the receptors were prepared with appropriate charge assignments and parameter additions for the present metals. Molecular docking was performed using 100 runs in AutoDock 4.2 [20], applying default parameters with a population size of 1500 individuals. For the 3LN1 protein, the grid box size was set to 50 × 50 × 50 and centered at coordinates 30.29, −23.07, and −15.99; for 308Y, the grid box size was set to 60 × 66 × 60, centered at coordinates −2.24, 25.69, and −0.94.

Molecular dynamics simulations were conducted using NAMD 3.0 software [21], following the protocol described by Solis-Hernandez et al. [22].

3.3. General Procedure for Coupling

In a flask equipped with magnetic stirring and a dropping funnel, 1.1 equivalents of the corresponding methyl ester were dissolved in a THF/DMSO (9:1) mixture. To the resulting mixture, 2.5 equivalents of DIEA were added, and the reaction was stirred for 1 h at 0 °C. The mixture was then added dropwise via the dropping funnel to a second flask containing 1 equivalent of δ-keto acid or δ-keto acid-AA-OH dissolved in THF, which has been pre-treated with 2 equivalents of DIEA and 1.1 equivalents of *i*BBCl. The reaction was allowed to proceed for 1 h at 0 °C and then at room temperature for 18 h. After the reaction was complete, the solvent was evaporated, and the product was extracted with AcOEt (3 × 50 mL). The organic phase was washed with HCl 10% solution and a saturated $NaHCO_3$ solution. The organic layer was dried over anhydrous Na_2SO_4. Purification was carried out as described in each case.

3.4. Espectral Data for Best Results

(4-(4-methoxyphenyl)-4-oxobutanoyl)-*L*-phenylalanine (**3**). ^{1}H NMR (400 MHz, CD_3OD TMS) δ ppm: 7.90 (d, *J* = 8.8 Hz, 2H), 7.16 (m, 5H), 6.95 (d, *J* = 8.8 Hz, 2H), 4.53 (dd, *J* = 8.0, 4.9 Hz, 1H), 3.83 (s, 3H), 3.21 (dd, *J* = 13.8, 4.8 Hz, 1H), 3.13 (td, *J* = 6.9, 3.9 Hz, 2H), 2.95 (dd, *J* = 13.7, 8.1 Hz, 1H), 2.52 (t, *J* = 6.9 Hz, 2H). ^{13}C NMR (100 MHz, CD_3OD) δ 199.1, 174.8, 165.2, 138.4, 131.4, 130.8, 130.3, 129.3, 127.7, 114.8, 56.0, 55.1, 38.5, 34.5, 30.7.

(4-(4-methoxyphenyl)-4-oxobutanoyl)-*L*-tyrosine (**4**). ^{1}H NMR (400 MHz, $CDCl_3$, TMS) δ ppm: 7.93 (d, *J* = 8.9 Hz, 2H), 7.05 (d, *J* = 8.5 Hz, 2H), 6.98 (d, *J* = 8.9 Hz, 2H), 6.69 (d, *J* = 8.5 Hz, 2H), 4.61 (dd, *J* = 8.6, 5.3 Hz, 1H), 3.85 (s, 3H), 3.15 (t, *J* = 7.0 Hz, 2H), 3.09 (dd, *J* = 14.0, 5.2 Hz, 1H), 2.86 (dd, *J* = 14.0, 8.6 Hz, 1H), 2.56 (td, *J* = 7.0, 1.6 Hz, 1H).^{13}C NMR (100 MHz, CD_3OD) δ ppm: 199.1, 174.9, 174.8, 165.2, 157.2, 131.4, 131.3, 130.8, 129.0, 116.1, 114.8, 56.0, 55.2, 37.7, 34.5, 30.7.

methyl (4-(4-methoxyphenyl)-4-oxobutanoyl)-*L*-tyrosyl-*L*-phenylalaninate (**7**). ^{1}H NMR (400 MHz, CD_3OD) δ 8.23–8.10 (m, 1H), 7.95 (d, *J* = 8.9, 2H), 7.28–7.15 (m, 4H), 7.04–6.97 (m, 4H), 6.66 (d, *J* = 8.9, 2H), 4.68–4.61 (m, 1H), 4.57–448 (m, 1H), 3.86 (s, 3H), 3.58 (s, 3H), 3.24–3.11 (m, 3H), 3.07–2.96 (m, 2H), 2.74–2.64 (m, 1H), 2.59–2.37 (m, 2H). ^{13}C NMR (101 MHz, CD_3OD) δ 199.6, 175.1, 173.7, 173.0, 165.4, 157.1, 138.0, 131.5, 131.2, 130.7, 130.3, 129.5, 129.1, 127.8, 116.1, 114.8, 56.1, 56.0, 55.2, 52.6, 38.3, 37.7, 34.7, 30.8.

4. Conclusions

The succesful synthesis of hybrid compounds **3**, **4** y **7** sets the stage for their exploration and potential use as anti-inflammatory agents, given their significant interactions with their pharmacological targets and results comparable to the reference drug. These findings highlight them as promisin candidates, offering a foundation for the development of a new generation of drugs with dual action on two key enzymes, COX and LOX, implicated in chronic degenerative diseases.

Author Contributions: All authors contributed equally to this work. All authors have read and agreed to the published version of the manuscript.

Funding: We are indebted to Coordinación de la Investigación Científica (CIC), Universidad Michoacana de San Nicolás de Hidalgo, for financial support. We also thank Consejo Nacional de Humanidades, Ciencias y Tecnologías (CONAHCYT, Mexico) for financial support via grants 252239 and IXM 4933.

Institutional Review Board Statement: Not applicable.

Informed Consent Statement: Not applicable.

Data Availability Statement: The datasets presented in this article are not readily available because the data are part of an ongoing study. Requests to access the datasets should be directed to J.A.A.-V.

Conflicts of Interest: The authors declare no conflicts of interest.

References

1. Dinarello, C.A. Proinflammatory cytokines. *Chest* **2000**, *118*, 503–508.
2. Passos, F.R.S.; Heimfarth, L.; Monteiro, B.S.; Correa, C.B.; de Moura, T.R.; de Souza Araújo, A.A.; Martins-Filho, P.R.; Quintans-Júnior, L.J.; Quintans, J.D.S.S. Oxidative stress and inflammatory markers in patients with COVID-19: Potential role of RAGE, HMGB1, GFAP and COX-2 in disease severity. *Int. Immunopharmacol.* **2022**, *104*, 108502–108509.
3. Ayola-Serrano, N.C.; Roy, N.; Fathah, Z.; Anwar, M.M.; Singh, B.; Ammar, N.; Sah, R.; Elba, A.; Utt, R.S.; Pecho-Silva, S.; et al. The role of 5-lipoxygenase in the pathophysiology of COVID-19 and its therapeutic implications. *Inflamm. Res.* **2021**, *70*, 877–889.
4. Hoxha, M. A systematic review on the role of eicosanoid pathways in rheumatoid arthritis. *Adv. Med. Sci.* **2018**, *63*, 22–29.
5. Almutairi, K.; Nossent, J.; Preen, D.; Keen, H.; Inderjeeth, C. The global prevalence of rheumatoid arthritis: A meta-analysis based on a systematic review. *Rheumatol. Int.* **2021**, *41*, 863–877.
6. Rudrapal, M.; Eltayeb, W.A.; Rakshit, G.; El-Arabey, A.A.; Khan, J.; Aldosari, S.M.; Alshehri,B.; Abdalla, M. Dual synergistic inhibition of COX and LOX by potential chemicals from Indian daily spices investigated through detailed computational studies. *Sci. Rep.* **2023**, *13*, 8656.
7. Che, X.H.; Chen, C.L.; Ye, X.L.; Weng, G.B.; Guo, X.Z.; Yu, W.Y.; Tao, X.; Chen, Y.C.; Chen, X. Dual inhibition of COX-2/5-LOX blocks colon cancer proliferation, migration and invasion in vitro. *Oncol. Rep.* **2016**, *35*, 1680–1688.
8. Rajakrishnan, V.; Manoj, V.R.; Rao, G.S. Computer-aided, rational design of a potent and selective small peptide inhibitor of cyclooxygenase 2 (COX2). *J. Biomol. Struct. Dyn.* **2008**, *25*, 535–542.
9. Hong, Y.I.N.; PAN, X.C.; WANG, S.K.; YANG, L.G.; SUN, G.J. Protective effect of wheat peptides against small intestinal damage induced by non-steroidal anti-inflammatory drugs in rats. *J. Integr. Agric.* **2014**, *13*, 2019–2027.
10. Mariniello, D.F.; Allocca, V.; D'Agnano, V.; Villaro, R.; Lanata, L.; Bagnasco, M.; Bianco, A.; Perrotta, F. Strategies tackling viral replication and inflammatory pathways as early pharmacological treatment for SARS-CoV-2 infection: Any potential role for ketoprofen lysine salt? *Molecules* **2022**, *27*, 8919.
11. Jorge-Aarón, R.M.; Rosa-Ester, M.P. N-acetylcysteine as a potential treatment for COVID-19. *Future Microbiol.* **2020**, *15*, 959–962.
12. Mohanty, R.R.; Padhy, B.M.; Das, S.; Meher, B.R. Therapeutic potential of N-acetyl cysteine (NAC) in preventing cytokine storm in COVID-19: Review of current evidence. *Eur. Rev. Med. Pharmacol. Sci.* **2021**, *25*, 2802–2807.
13. Tiwari, A.D.; Panda, S.S.; Girgis, A.S.; Sahu, S.; George, R.F.; Srour, A.M.; La Starza, B.; Asiri, A.M.; Hall, C.D.; Katritzky, A.R. Microwave assisted synthesis and QSAR study of novel NSAID acetaminophen conjugates with amino acid linkers. *Org. Biomol. Chem.* **2014**, *12*, 7238–7249.
14. Moreira, R.; Jervis, P.J.; Carvalho, A.; Ferreira, P.M.; Martins, J.A.; Valentão, P.; Andrade, P.B.; Pereira, D.M. Biological evaluation of naproxen–dehydrodipeptide conjugates with self-hydrogelation capacity as dual LOX/COX inhibitors. *Pharmaceutics* **2020**, *12*, 122–140.
15. Li, J.; Kuang, Y.; Gao, Y.; Du, X.; Shi, J.; Xu, B. D-amino acids boost the selectivity and confer supramolecular hydrogels of a nonsteroidal anti-inflammatory drug (NSAID). *J. Am. Chem. Soc.* **2013**, *135*, 542–545.
16. Li, J.; Kuang, Y.; Shi, J.; Gao, Y.; Zhou, J.; Xu, B. The conjugation of nonsteroidal anti-inflammatory drugs (NSAID) to small peptides for generating multifunctional supramolecular nanofibers/hydrogels. *Beilstein J. Org. Chem.* **2012**, *9*, 908–917.
17. Elhenawy, A.A.; Al-Harbi, L.M.; Moustafa, G.O.; El-Gazzar, M.A.; Abdel-Rahman, R.F.; Salim, A.E. Synthesis, comparative docking, and pharmacological activity of naproxen amino acid derivatives as possible anti-inflammatory and analgesic agents. *Drug Des. Dev. Ther.* **2019**, *13*, 1773–1790.
18. Jiménez-Cruz, J.C.; Guzmán-Mejía, R.; Juaristi, E.; Sánchez-Antonio, O.; García-Revilla, M.A.; González-Campos, J.B.; Aviña-Verduzco, J. Preparation of aromatic γ-hydroxyketones by means of Heck coupling of aryl halides and 2, 3-dihydrofuran, catalyzed by a palladium (ii) glycine complex under microwave irradiation. *New J. Chem.* **2020**, *44*, 13382–13392.
19. Chaudhary, N.; Aparoy, P. Application of per-residue energy decomposition to identify the set of amino acids critical for in silico prediction of COX-2 inhibitory activity. *Heliyon* **2020**, *6*, e04944.
20. Morris, G.M.; Huey, R.; Lindstrom, W.; Sanner, M.F.; Belew, R.K.; Goodsell, D.S.; Olson, A.J. AutoDock4 and AutoDockTools4: Automated docking with selective receptor flexibility. *J. Comput. Chem.* **2009**, *30*, 2785–2791.
21. Phillips, J.C.; Hardy, D.J.; Maia, J.D.; Stone, J.E.; Ribeiro, J.V.; Bernardi, R.C.; Buch, R.; Fiorin, G.; Hénin, J.; Jiang, W.; et al. Scalable molecular dynamics on CPU and GPU architectures with NAMD. *J. Chem. Phys.* **2020**, *153*, 044130.
22. Solís-Hernández, M.D.J.; Palomares-Báez, J.P.; Herrera-Bucio, R.; Chacón-García, L.; Navarro-Santos, P. (2023). Derivates of 1, 6-dihyadroazaazulenes as inhibitors of tyrosine kinases BCR-ABL1 wild type and mutant T315I: A molecular dynamics approach. *J. Biomol. Struct. Dyn.* **2023**, *2023*, 2279274.